EVALUATION OF VARIOUS DESIGN METHODS FOR PREDICTING REINFORCEMENT LOADS WITHIN TWO DIFFERENT FACING STIFFNESS GEOSYNTHETIC-REINFORCED SOIL STRUCTURES

T. L. Liu[1], and K. H. Yang[2]
[1]Graduate Student, Department of Construction Engineering, National Taiwan University of Science and Technology; Tel: +886-9 213 19786; Email: melody0039@gmail.com,
[2]Assistant Professor, Department of Construction Engineering, National Taiwan University of Science and Technology; Tel: +886-2 273 01227; Fax: +886-2 273 76606; Email:khy@mail.ntust.edu.tw

ABSTRACT

Proper estimation of reinforcement loads is a key to evaluate the internal stabilities of Geosynthetic-Reinforced Soil (GRS) structures. Prediction methods for reinforcement loads within GRS structures in current practice can be categorized into two approaches: force equilibrium approach (i.e., earth pressure method and limit equilibrium method) and deformation based approach (i.e., K-stiffness method and finite element method). Until today, the effects of these methods have not been extensively examined and compared yet. In this paper, the reinforcement loads measured from two full-scale and carefully instrumented GRS walls are used to examine the prediction of reinforcement loads by the aforementioned methods. These walls are 3.6m high with different facing stiffness; one wall was constructed with a stiffer segmental modular block face and the other with a flexible wrapped-around face. Comparison results from both wall cases indicate the force equilibrium approach overly predict the reinforcement loads. The K-stiffness method shows an obvious underestimate under surcharging conditions. The finite element predictions are sufficiently accurate under working stress conditions but do not successfully predict the measured reinforcement loads under large loading conditions. Furthermore, a stiff facing in a reinforced soil wall can restrain wall deformation and thus result in significant reductions in reinforcement loads compared to the flexible facing system. However, the influence of facing stiffness is typically not accounted for in the force equilibrium approach, so that the force equilibrium approach significantly overestimates reinforcement loads for the stiff face wall. Reasons of discrepancy between predicted reinforcement loads and measured data are discussed. The results obtained from this study provide insightful information for the design of GRS structures.

Keywords: Geosynthetic-reinforced soil structure, facing stiffness, reinforcement load, force-equilibrium, deformation.

INTRODUCTION

Mechanical Stabilized Earth (MSE) retaining structures are now widely used in various projects including residences, highways, bridge abutments, and slope stabilization for the purposes as increasing Right of Way (ROW), resisting earth pressures, and providing load bearing on top of MSE structures, and allowing for changes of elevation in highway projects. A number of factors have propelled the acceptance of MSE retaining structures, including aesthetics, reliability, and low cost. Moreover, good construction techniques, impressive seismic performances, and a striking ability to withstand large deformations without structural distress account for MSE structures desirability. The design of MSE retaining structures is the result of a synergistic approach in the current MSE structure design guidelines (AASHTO 2002, Elias et al. 2001, NCMA 2010). Figure 1 shows the wall system analysis for internal, external, global and seismic stability as well as deformability. MSE structures must meet certain factors of safety, *FS*, against all failure models.

In analyzing the internal stability of GRS structures, it is require to predict the maximum reinforcement tensile load, T_{max}, in each reinforcement layer. The knowledge of the forces in the reinforcements enables one to select reinforcements having adequate long-term strength (against breakage), to calculate the length required to resist pullout within the stable soil zone (against pullout), and to calculate the required connection strength at facing (against connection failure). As a result, the evaluation of T_{max} is a key for the internal stability analyses of MSE structures. Prediction methods for reinforcement loads within GRS structures in current research and practice can be categorized into two approaches: force equilibrium approach (i.e., earth pressure method and limit equilibrium method) and deformation-based approach (i.e., K-stiffness method and finite element method). However, until today, the accuracy of these methods has not been extensively

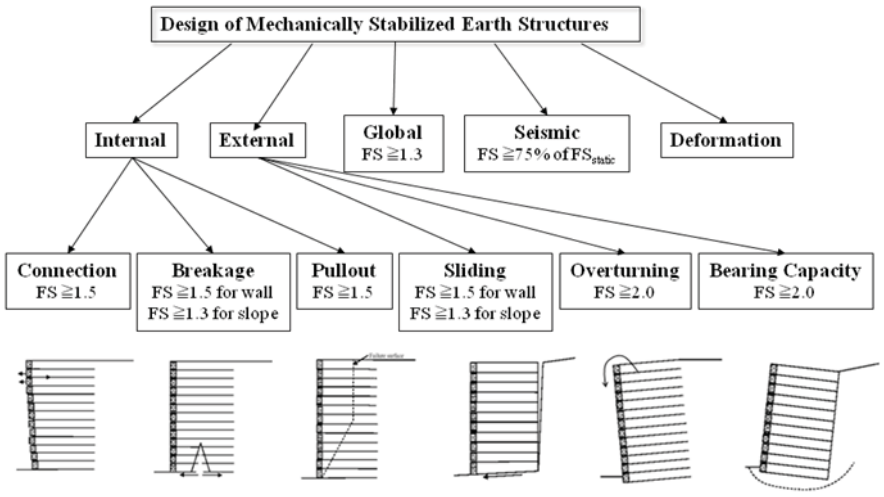

Fig. 1 Failure modes and safety factors for the design of MSE structures as required by FHWA (2001)

examined evaluated yet. In addition, reinforced soil walls commonly include facing elements that may act to increase the system stability and result in reducing the requirements of reinforcement loads for equilibrium. However, the current design procedures do not consider this structural contribution of the facing to the reduction of reinforcement loads.

Accordingly, the observation above has prompted the current study to examine the effects of these methods to predict reinforcement loads T_{max} within GRS structures. The accuracy of each method is examined by comparing the predicted T_{max} with the measured T_{max} from two full-scale (3.6m high) and carefully instrumented GRS walls with different facing stiffness. Reasons of discrepancy between predicted and measured T_{max} are discussed. Results obtained from this study are expected to provide insightful information for the design of GRS structures.

FULL-SCALE GRS WALL TESTS

Two full-scale GRS walls were conducted by Bathurst et al. (2006) in the Royal Military College (RMC); one was constructed with a stiff segmental modular block face and the other one with a flexible wrapped-around face. Both GRS walls are 3.6m high with 6 reinforcement layers at a spacing of S_v=0.6m and facing slope of ω=8°. Figure 2 illustrates the cross-section of the GRS test walls. It should be noted that different from a typical wrapped-face GRS wall that each facing wrap was extended back into the reinforced soil zone, each facing wrap in the flexible wall was attached to the reinforcement layer above using a metal bar clamp to form the wall face.

The backfill, named RMC sand, is a clean, uniform graded, beach sand classified as poor sand (SP) according to USCS. The backfill soil has D_{50}=0.34mm, coefficient of curvature C_c= 2.25, co-

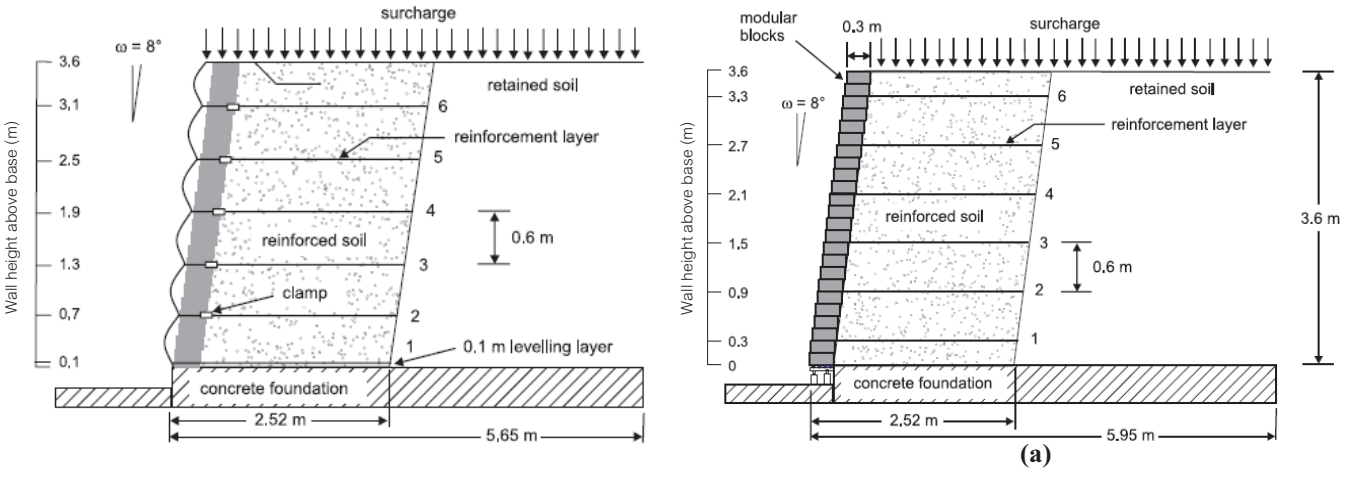

Fig. 2 Cross-section of the GRS test wall: (a) flexible wrapped face wall; (b) stiff segmental face wall (Bathurst et al. 2006)

efficient of uniformity C_u=1.09, unit weight γ=16.7kN/m^3 and soil peak friction angle ϕ_{tx}=35^o by triaxial compression tests and ϕ_{ps}=42^o by plane strain tests. The reinforcement is a polypropylene geogrid with a total length of 2.52m measured from the front wall face. The ultimate tensile strength was T_{ult}=13 kN/m obtained from the wide width strip tensile test . Because the reinforcement strain rate (10%/min) in the wide width tensile test is much larger than the strain rate possibly developing in the test wall, a series of constant-load creep tests were carried out by Bathurst et al. (2006) to determine the isochronous load-strain responses of reinforcement at 1000hr, similar to the duration of the wall test. The stress-strain-volumetric responses of RMC sand and the isochronous load-strain responses of reinforcement are discussed later.

After completion of wall construction, uniform surcharges were applied on top of the wall with load increment of 10kPa until final loading of 80kPa was reached. These walls were intensively and carefully instrumented to measure the performance of the wall at the end of construction and during staged uniform surcharging; for instance, the strain gauges and extensometers attached to reinforcements were used to measure the reinforcement strains along each reinforcement layer. The measured maximum reinforcement strain at each reinforcement layer then multiplied by the reinforcement secant stiffness (T_{max}=$J(\varepsilon)$xε) determined from the isochronous load-strain responses at the same strain level to estimate the mobilized reinforcement loads in the test walls.

PREDICTION OF T_{MAX}

Earth Pressure Method

Earth pressure method has been adopted in many current design guidelines (AASHTO 2002, Elias et al., NCMA 2010) to predict reinforcement loads of MSE walls. The design rationale assumes the tensile forces developed in reinforcements are in local equilibrium with the lateral earth pressure generated in MSE walls. FHWA design guidelines recommend using Eq. 1 to predict T_{max} of each reinforcement layer.

$$T_{\max} = \left(\frac{k_r}{K_a} \right) K_a (\gamma z + q) S \qquad (1)$$

where T_{max} is the maximum reinforcement load in each reinforcement layer; k_r/K_a is the normalized lateral earth pressure coefficient; K_a is the theoretical Rankine or Coulomb active earth pressure coefficient; γ is the backfill unit weight; z is the depth below the top of the backfill, q is the surcharge, S_v is the tributary area (equivalent to the reinforcement vertical spacing when analyses are carried out per unit length of wall). The k_r/K_a varies with the type of reinforcements; for flexible MSE walls or GRS walls, the k_r/K_a has a value of 1.0 and remains constant throughout the depth of the wall. This implies that for flexible MSE walls or GRS walls the horizontal movement occurring during construction is sufficient for the soil to reach active stress state and generate active earth pressure. The final computed reinforcement tensile loads increases linearly from the topmost layer of reinforcement to the bottommost layer of reinforcement (proportional to the overburden pressure).

The earth pressure method is used in this study to predict the T_{max} developed within the two full-scale GRS walls at various loading conditions. Because the test walls have no backslope, K_a in Equation 1 can be calculated according to Rankine and Coulomb theories, as shown in Eqs: 2 and 3, respectively.

$$K_a = \tan^2 (45 - \frac{\phi}{2}) \qquad (2)$$

$$K_a = \frac{\cos^2 (\omega + \phi)}{\cos^2 \omega \cos(\delta - \omega) \left[1 + \sqrt{\frac{\sin(\phi + \delta) \sin \phi}{\cos(\delta - \omega) \cos \omega}} \right]^2} \qquad (3)$$

where ϕ is the backfill friction angle; ω is the facing batter; δ is the soil-facing interface friction angle. Different from Rankine theory, Coulomb theory is capable to account for the effect of wall facing batter and soil-face interaction on K_a, resulting in the calculated K_a is less than the K_a from Rankine theory. The peak plane strain friction angle of ϕ_{ps}=42^o was inputted into Eqs 2 and 3 to characterize the backfill shear strength in the test wall conditions. For Coulomb theory, δ=ϕ was used for both walls, assuming the facing column creates a soil-to-soil interface for the flexible face wall and the soil-facing block interface friction is controlled by the peak soil friction angle for the stiff face wall. The normalized lateral earth pressure coefficient of k_r/K_a equate to 1 is applied for the GRS test wall. Input values for other parameters in Equation 1 correspond to the physical wall test.

Limit Equilibrium Method

Limit equilibrium method has been used to analyze slope stability for many years by assuming the soil at failure obeys the perfectly plastic Mohr-Coulomb criterion and searching for a critical failure surface that contains a minimum factor of safety.

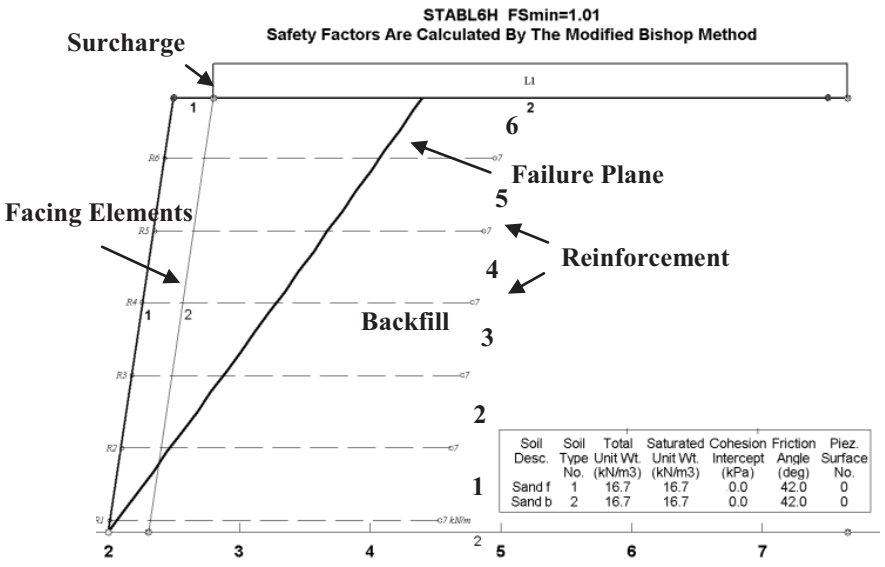

Fig. 3 Limit equilibrium model and results of the GRS test wall

Limit equilibrium analyses of the reinforced soil structures have also been successfully reported (Zornberg et al. 1998). The stabilizing forces contributed by the reinforcement loads are incorporated into the equilibrium equation (balance of force or moment) at "limit" state (right between stable and instable sates).

In this study, limit equilibrium analyses were performed using the Modified Bishop method with circular surfaces as coded in the commercial slope stability analysis software, STEDwin. Figure 3 shows the limit equilibrium modeling of the GRS test wall. The wall configuration and reinforcement layout of the limit equilibrium model follows the physical test wall. The peak plane strain friction angle of $\phi_{ps}=42^o$ was used. The facing elements (i.e., wrapped face or segmental modular face) did not be included in the calculation. The discrepancy between predicted and measured reinforcement loads due to the ignorance of facing stiffness is discussed later. The limit equilibrium analysis assumed that the reinforcement forces had a uniform distribution with depth and considered the contribution of geogrid overlap layers to system stability. Unlike the recommended use of allowable tensile strength in the conventional analysis, the limit equilibrium analyses in this study did not consider reduction factors due to installation damage, creep or degradation (i.e., all reduction factors were 1.0). A series of uniform loadings were applied on the top of limit equilibrium model to simulate the surcharges. The mobilized reinforcement loads T_{max} at different surcharges were determined by varying the values of T_{max} until FS=1 was reached at each surcharge level.

K-Stiffness Method

Allen et al. (2003) and Bathurst et al. (2005, 2008) proposed a new working stress method for estimation of reinforcement loads in GRS walls, known as K-stiffness method. In the development of the K-stiffness method, a database of 30 wall case studies was used to establish an empirical expression to predict T_{max} at each reinforcement layer. The K-stiffness method has altered the conventional equation, Eq. 1, for computing T_{max} by adding many influence factors Φ, calculated as:

$$T_{\max} = \frac{1}{2} K_o (\gamma H + q) S_v D_{t\max} \Phi \tag{4}$$

$$\Phi = \Phi_g \Phi_{local} \Phi_{fs} \Phi_{fb} \Phi_c \tag{5}$$

where *Tmax* is the maximum reinforcement load; *Ko* is the at-rest earth pressure coefficient; γ is the backfill unit weight; H is the wall height, q is the surcharge; S_v is the tributary area or the reinforcement vertical spacing; D_{tmax} is the load distribution factor; Φ is the influence factor that is the product of factors that account for the effects of global and local reinforcement stiffness Φ_g and Φ_{local}, facing stiffness Φ_{fs}, face batter Φ_{fb}, and backfill cohesion Φ_c.

In this study, the peak plane strain friction angle of $\phi_{ps}=42^o$, as suggested by the K-stiffness method, was used in the calculation. The reinforcement stiffness at 2% strain of $J_{2\%}$=100kN/m, determined from the project-specific isochronous load-strain response, was applied to calculate the influence factor for the effects of global and local reinforcement

stiffness (i.e., Φ_g =0.283 and Φ_{local}=1, respectively). The facing stiffness of Φ_{fs}=1 and 0.35 are applied for the wrapped face wall and segmental modular face wall according to the recommendation in the K-stiffness method. Use of Φ_{fs}=1 for the wrapped face wall implies the wrapped-around face has no influence on T_{max}. Specifically, the wrapped-around face dose not reduce the reinforcement loads in the K-Stiffness method. The calculated Φ_{fb}=0.93 is applied to account for the effect of facing slope (ω=8°) on T_{max}. Because there is no cohesion in the backfill, the effect of cohesion is not considered in the calculation (i.e., Φ_c=1). Input values for other parameters in Eqs. 4 and 5 correspond to the physical test wall values.

Finite Element Method

Finite element method has been widely applied to model the behavior of GRS structures (e.g., Huang et al. 2009, Hatami and Bathurst 2005, 2006, Karpurapu and Bathurst 1995, Ling et al. 2000, Lopes et al. 1994). Analysis based on finite element method considers full continuum mechanics, e.g., the constitutive relationships of all materials involved. It can represent a problem in the most realistic fashion, and its prediction of performance can be quite accurate. In this study, the finite element program, PLAXIS version 8.2 (PLAXIS 2005), was used to develop a numerical model for the flexible face wall. Figure 4 shows the finite element model of the flexible wrapped face wall. The finite element modeling of the stiff face wall was not performed in this study. The finite element results were directly obtained from Hatami and Bathurst (2005, 2006) and Huang et al. (2009) who conducted a series of finite element studies using the modified Duncan-Change Hyperbolic model to simulate the behavior of the same stiff face wall under working stress and loading conditions.

The FE modeling of the flexible face wall is discussed as follows. The backfill, RMC sand, was modeled as a stress-dependent, hyperbolic elasto-plastic material using the Hardening Soil model. Table 1 lists the material properties of RMC sand. Figure 5 show the calibration results of stress-strain-volumetric response of RMC sand. A small cohesion value, c=1 kPa and 2kPa were introduced in the soil model at construction and during staged uniform surcharging, respectively, to improve numerical stability. In addition, because each facing wrap was fixed using a metal bar clamp in the test wall, a cohesion of c=10 kPa was applied to the soil elements in the wrapped-around face to simulate this effect. The reinforcements were modeled as elasto-plastic bar elements with an axial stiffness EA, maximum axial tensile strength, N_p and no compressive strength. Table 1 lists the reinforcement properties determined from the isochronous load-strain response at 1000hr. Figure 6 show the calibration results of geogrid load-strain response. Note that in order to model the nonlinear load-strain response, the reinforcement stiffness were inputted as EA= 100kN/m and 70kN/m for construction and during staged uniform surcharging, respectively. These input values of reinforcement stiffness correspond to the average mobilized reinforcement strain of 2% at construction and 7% during staged uniform surcharging.

Stage construction was included in the simulation by conducting layer-by layer construction in PLAXIS. The uniform surcharges were applied on the top of the finite element model with load increment of 10kPa until target loading of 80kPa was reached. Updated mesh was activated to account for large deformations, especially important at significant loading conditions. Notably, the calculated FE failure was earlier than the actual failure of soil, in which a clear internal failure surface was observed in the test wall at q=90kPa. The FE simulation terminated at the next 10kPa loading increment after completing 40kPa due to numerical difficulties occurred in the computation. Inspection of soil elements at the termination of simulation revealed that most of soil elements along the failure surface reached their peak shear strength. That may cause the numerical instability in the simulation and result in the termination of simulation. Last, the accuracy of the numerical model was verified by quantitatively comparing the reinforcement strains along each layer and the comparison results showed the prediction and measurement were in satisfactory agreement.

RESULTS AND DISCUSSIONS

Results

The accuracy of each method is examined by comparing the predicted T_{max} with the measured T_{max} from the test walls. Figures 7 show the comparison of T_{max} at the end of construction (q=0kPa) for both wall cases. The "measurement" in Fig. 7, indicates the "measured" reinforcement load calculated by multiplying the measured strain by the isochronous stiffness value at the same strain level for each reinforcement layer. The range bars in Fig. 7 represent 10% of uncertainties on measured T_{max} to account for the estimate error of the strain measurements and isochronous stiffness values. Comparison results indicate the earth pressure methods using both Rankine and Coulomb theories overly predict the reinforcement loads for both wall cases. The earth pressure method using Coulomb theory is considered superior to the one using Rankine theory because Coulomb theory can account for the effect of wall facing batter and soil-face interaction on K_a.

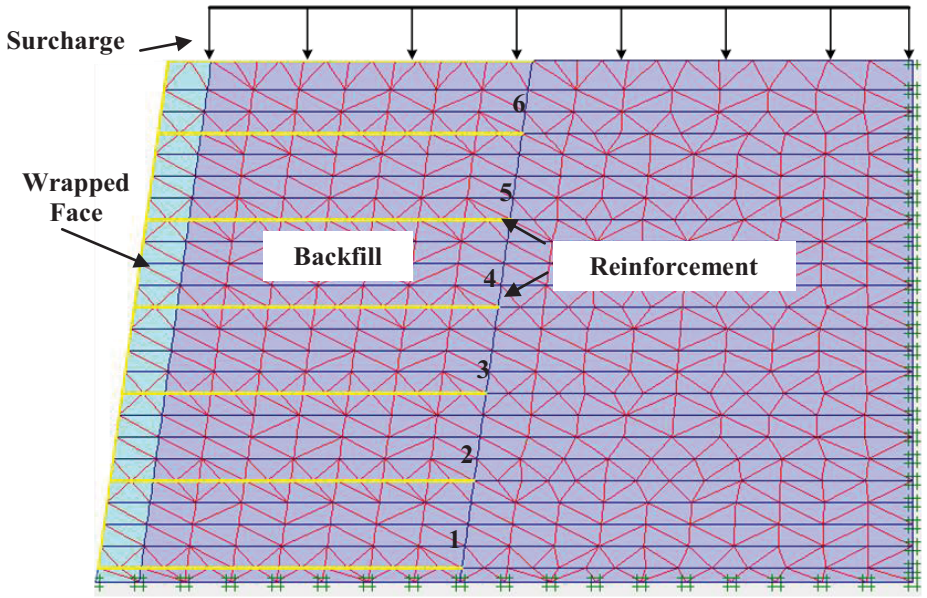

Fig. 4 Finite element model of the flexible wrapped face wall

Table 1 Material properties for RMC sand and geogrid

Material	Value
Backfill	
γ (unit weight) (kN/m^3)	16.7
ϕ (peak friction angle) (degree)	42
c (cohesion) (kPa)	1 for construction 2 for surcharging 10 for wrapped-around face
ψ (dilation angle) (degree)	11
E_{50}^{ref} (secant stiffness) (kPa)	6.2x10^4
E_{50}^{ref} (tangent stiffness for primary odeometer loading) (kPa)	6x10^4
E_{ur}^{ref} (unloading/reloading stiffness) (kPa)	1.8x10^5
m (modulus exponent)	0.5
R_f (failure ratio)	0.8
Reinforcement	
N_p (maximum tensile strength) (kN/m)	7.7
EA (axial stiffness) (kN/m)	100 for construction 70 for surcharging

Note: E_{ur}^{ref} was assumed to be $3E_{50}^{ref}$ as the default setting in PLAXIS

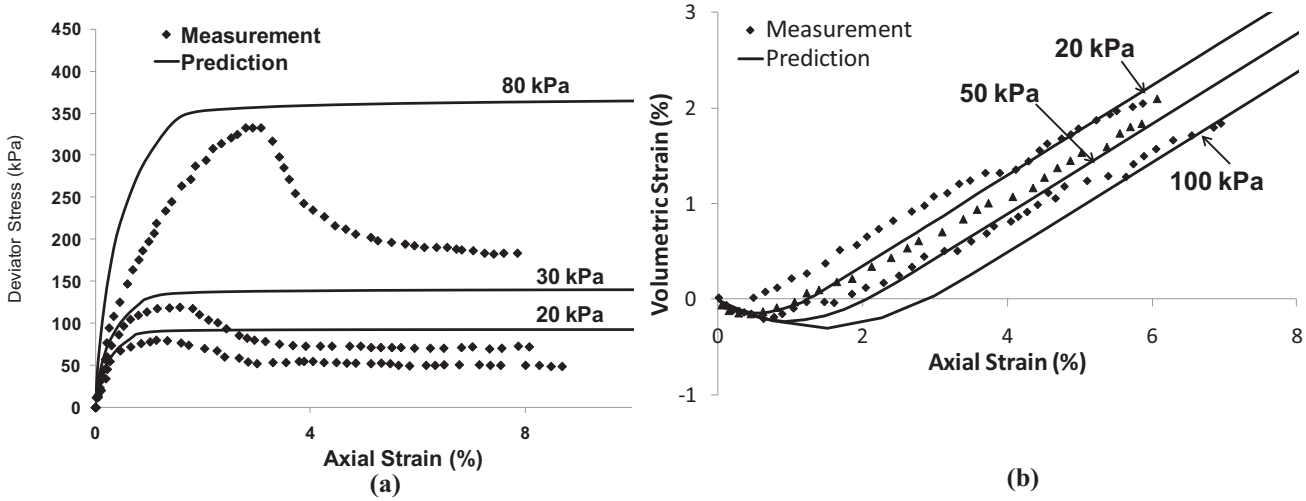

Fig. 5 Measured and predicted stress-strain-volumetric response of RMC sand: (a) stress-strain response from plane strain tests; (b) axial strain-volumetric strain from triaxial tests. Note that no volumetric strain response was taken in plane strain tests.

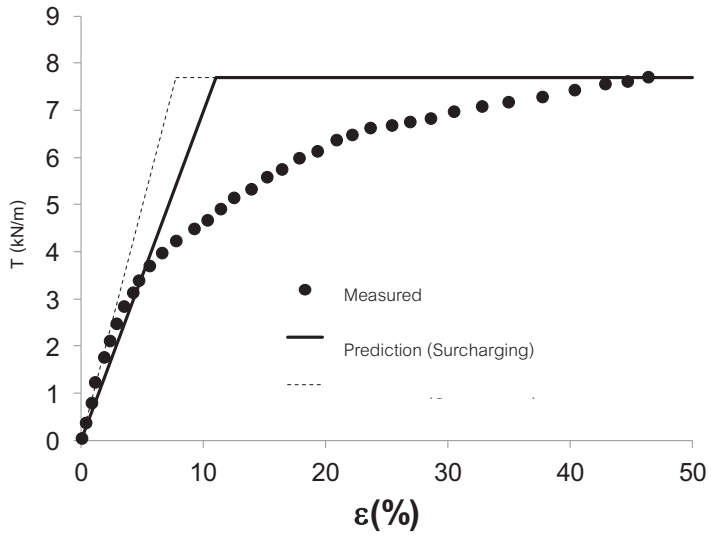

Fig. 6 Measured and predicted load-strain response of geogrid

The T_{max} predicted by the limit equilibrium method for the flexible face wall is in a good agreement with the maximum value of the measured T_{max}. However, the uniform distribution of reinforcement load with depth assumed in the limit equilibrium method does not match the distribution of measured data. The limit equilibrium method excessively predicts the T_{max} for the stiff face wall. The K-stiffness method slightly underestimates the measured T_{max} for the flexible face wall but seems to show a good prediction for the stiff face wall. The finite element predictions are sufficiently accurate compared with the measured T_{max} for both wall cases.

Figure 8 show the summation of reinforcement loads T_{max} from all reinforcement layers at various surcharge levels for both wall cases. The measured ΣT_{max} from the strain magnitude and distribution in the six layers of reinforcements at the end of construction, q=40kPa and q=80kPa, reported by Bathurst et al. (2006) and Hatami and Bathurst (2006), are plotted in Figure. 8. Overall, each method is able to predict the increase of ΣT_{max} with increasing surcharges. However, the force equilibrium approach, including the earth pressure methods using Rankine and Coulomb theories and the limit equilibrium method, overly predicts the ΣT_{max} at different surcharge levels for both wall cases. The magnitude of the discrepancy between predicted and measured results increases as the surcharge increases.

As for the deformation-based approach, the K-stiffness method is in a good agreement with the

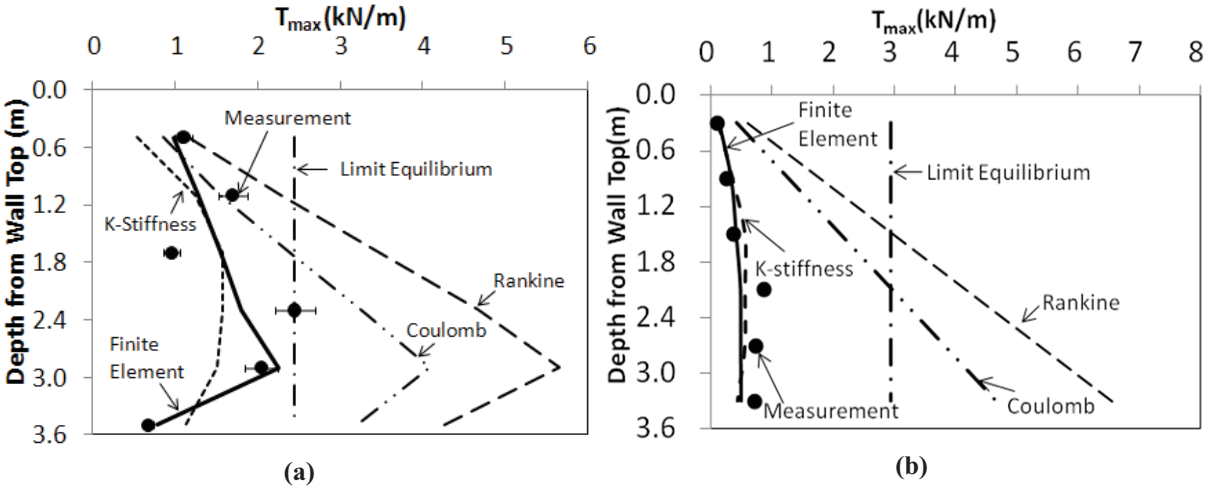

Fig. 7 Comparison of reinforcement load T_{max} at each reinforcement layer at the end of construction (q=0kPa): (a) flexible wrapped face wall; (b) stiff segmental face wall

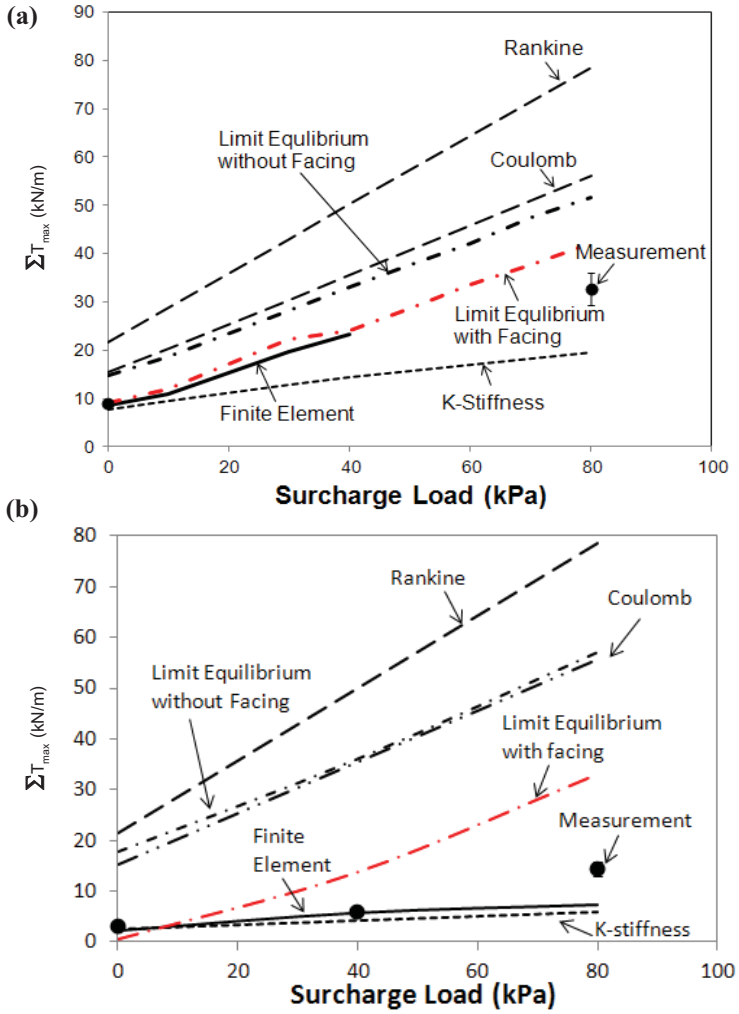

Fig. 8 Comparison of summation of reinforcement loads ΣT_{max} from all reinforcement layers at different sur charge levels: (a) flexible wrapped face wall; (b) stiff segmental face wall

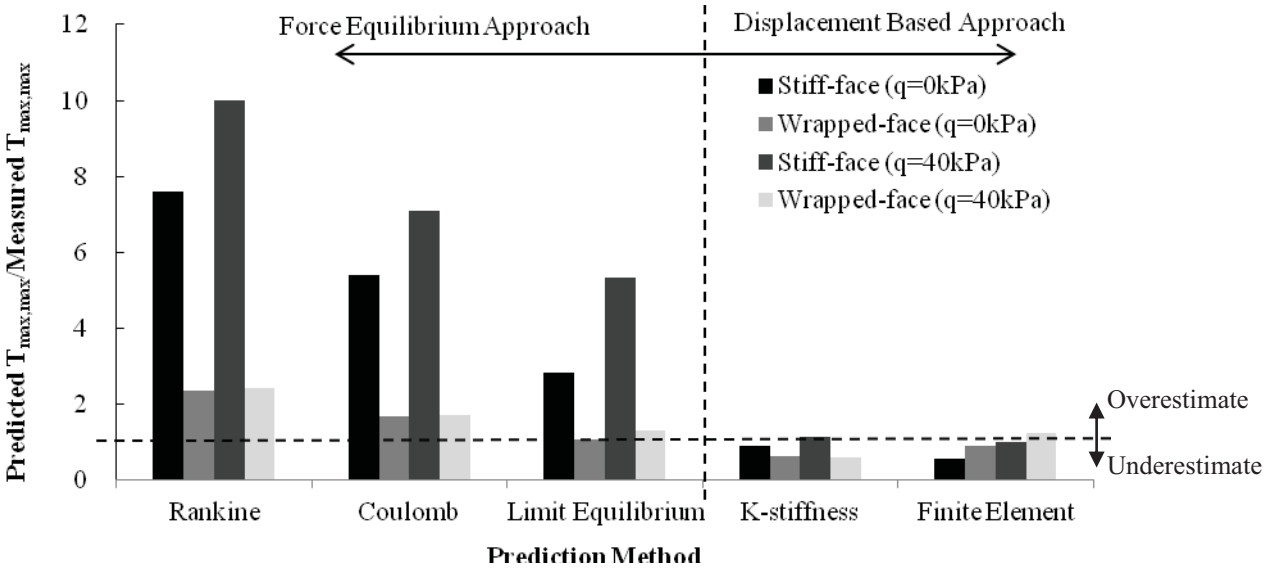

Fig. 9 Comparison of the maximum reinforcement load $T_{max,max}$ in the walls

measured ΣT_{max} under working stress conditions but shows an obvious underestimation under surcharging conditions. This observation is consistent with one of the limitations of the K-stiffness method discussed by Allen et al. (2003). Allen et al. (2003) demonstrated a good prediction of T_{max} for GRS walls under working stress conditions (developed soil strain ≤ soil failure strain, approximately 3%). However, for GRS structures under large surcharging conditions (developed soil strain > soil failure strain), the K-stiffness method consistently underpredicts T_{max}.

The finite element method agrees well with the measured data at q=0kPa but numerical illness occurs, as mentioned earlier, for the flexible face wall at large loading conditions (i.e., q≤40kPa). Therefore, the FE results for the flexible face wall are only presented until q=40kPa in Fig 8a. For the stiff face wall, the finite element predictions are sufficiently accurate at q≤40kPa but show an underestimate afterward. That is likely because the hyperbolic model used in the finite element simulation by Hatami and Bathurst (2005, 2006) and Huang et al. (2009) cannot capture the post-peak softening behavior at large loading conditions.

Figure 9 shows the ratio of the predicted maximum reinforcement loads in the walls, $T_{max,max,}$ to the measured maximum reinforcement loads in the walls at different surcharge levels. To predict the value of $T_{max,max}$ accurately is very important because the value of $T_{max,max}$ is conventionally used to determine the reinforcement tensile strength in the design of GRS wall internal stability against reinforcement breakage. We can observe from Figure 9 that the earth pressure method using Rankine theory has the most significant overestimate of $T_{max,max}$ value for the stiff face wall. The overestimate ratio is about of 8 to 10 from q=0kPa to 40kPa. In contrast, the K-stiffness method underestimates the $T_{max,max}$ value most significantly for the both flexible and stiff face walls with an average ratio of 0.7. The finite element method can predict the $T_{max,max}$ sufficiently accurate, except for the underestimate of $T_{max,max}$ value for the stiff face wall at q=0kPa. It may be worth pointing out that the limit equilibrium method can predict $T_{max,max}$ accurately for the flexible face wall, which the influence of facing stiff is relatively less compared to that from the stiff face wall.

Discussion on the Discrepancy

Holtz (2010) in the 46th Karl Terzaghi lecture discussed the discrepancy between predicted and measured T_{max} may generally come from:

1. Selection of soil shear strength properties to input into the prediction methods (*i.e.,* use $\phi_{triaxial}$, $\phi_{plane\ strain}$ or $\phi_{residual}$);
2. Error and uncertainty from field instrumentation and measurement;
3. Existence of apparent cohesion in the field unsaturated conditions; and
4. Influence of facing stiffness.

Above reasons were also discussed by other researches. For example, Leshchinsky (2009, 2010) used sand castle as an example to declare a trace of apparent cohesion from capillary suction or soil ma-

trix potential in the field unsaturated conditions may dramatically increase system stability and result in reducing the requirement of the T_{max} within GRS structures for equilibrium. Bathurst et al. (2006) compared the influence of facing stiffness on the measured reinforcement strain and commented that the wall facing is a structural element that acts to reduce the magnitude of deformations and reinforcement strains (or loads) of GRS structures.

For this study, the peak plane strain friction angle was used to characterize the backfill shear strength in the test walls because the test wall conditions conformed to the plane strain condition. Error and uncertainty from measurement and data interpretation were also considered using the range bar to represent the uncertainties on the measured T_{max}. The effect of apparent cohesion due to soil suction was not considered in the prediction of T_{max} in this study. This effect may be important for the field wall as discussed by Leshchinsky (2009, 2010); however, it is believed that this effect has insignificant influence on the measured T_{max} for the test walls discussed in this study. That is because the backfill used in the test wall was a uniform sand with relatively coarse sand particle (i.e., D_{50}=0.34mm) and less than 1% of fine soil. The backfill was compacted at a little moisture content of 3% to 5%. The apparent cohesion under this backfill condition is likely very little. To support above statement, an unconfined compression test, as shown in Figure. 10, was conducted to measure the magnitude of apparent cohesion of a sand specimen. The sand has the particle distribution and peak shear strength (classified as SP by USCS, D_{50}=0.3mm and ϕ_{tx}=35^o) similar to backfill used in the test walls and was compacted to the same water content and unit weight (ω=5% and γ=16.7kN/m^3) as the compaction conditions in the test walls. The rationale is that since saturated sand do not have any shear strength under unconfined condition, the soil shear strength measured from the unconfined compression test can be attributed to the effect of apparent cohesion due to soil suction. The measured unconfined compression strength of the sand specimen under previously described condition is approximately 3kPa, which suggests the apparent cohesion of the sand specimen has a very small value of approximately 1.5kPa.

The author's opinion, the facing stiffness as mentioned by Holtz (2010) and Bathurst et al. (2006) is the major source of conservatism in the force equilibrium approach to predict the T_{max}. However, the influence of facing stiffness is typically not accounted for in the current design procedures which are established based on the force equilibrium approach. To demonstrate the statement above, additional limit equilibrium analyses were conducted by inputting an additional cohesion of c=10 kPa to the soil elements in the wrapped-around face and a block-block interface strength of c_a=46 kPa and δ=57^o in the stiff face to simulate the effect of facing stiffness. These ways of modeling facing stiffness are similar to the finite element modeling as discussed in Section 3.4. The results of limit equilibrium analyses considering the effect of facing stiffness are shown in Fig. 8. The limit equilibrium results demonstrate modeling of facing stiffness in the limit equilibrium analysis can improve the prediction of ΣT_{max}. Some discrepancy between predicted and measured ΣT_{max} still can be observed in Fig. 8. That is because the effect of facing stiffness cannot be easily and quantitatively implemented in the force equilibrium method. More specifically, the effect of facing stiffness should also develop with increasing loadings instead of a constant value assumed in this study. Further studies are needed to more accurately simulate the effect of facing stiffness in the force equilibrium approach.

(a)

(b)

Fig. 10 Unconfined compression test to quantify the apparent cohesion of an unsaturated sand specimen: (a) before test; (b) failure of soil specimen

CONCLUSIONS

In this paper, the accuracy of various design methods to predict the reinforcement load T_{max} for each reinforcement layer was evaluated by comparing with the measured data from two full-scale and carefully instrumented GRS structures with different facing stiffness (i.e., flexible wrapped face wall and stiff segmental modular wall). Specific important conclusions and discussion points are summarized as follows.

- Comparison results indicate the force equilibrium approach overly predict the measured T_{max}, excpet that the limit equilibrium method can predict the maximum reinforcement loads in the walls, $T_{max,max,}$ accurately for the flexible face wall. Among all methods, the earth pressure method using Rankine theory has most significant overestimate of $T_{max,max}$ about of 8 to 10 from q=0kPa to 40kPa for the stiff face wall.
- The K-stiffness method shows an obvious underestimate of the measured T_{max} under large loading conditions for both wall cases. Among all methods, the K-stiffness method underestimates the $T_{max,max}$ value most significantly with an average ratio of 0.7.
- For the flexible wall, the finite element method agrees well with the measured data under working stress conditions but numerical illness occured earlier than the actual failure of structure at large loading conditions. For the stiff face wall, the finite element predictions are sufficiently accurate at $q \leq 40$kPa but show an underestimate afterward.
- The unconfined compression test results found the sand specimen, simialr to the backfill condition in the test walls, has a very little value of apparent cohesion (of approximately 1.5kPa), which would result in an insignificant influence on the measured T_{max} for the test walls.
- Ignorance of the effect of facing stiffness is the major source of conservatism in the force-equlibirum approach for the wall cases discussed in this study. That is becasue the facing stiffness can constraint system deforatiom and, consequently, decrease reinforcement loads, specially for the stiff face wall. This study demonstrated that modeling of facing stiffenss in the limit equilibirum anlaysis can improve the prediction of T_{max}. However, the influence of facing stiffness on the reduction of reinforcement loads cannot not be easily and quantitatively implemented in the force equilibrium method.

ACKNOWLEDGEMENTS

The financial support for this study was provided by the National Science Council of the Republic of China, Taiwan under Grant No. NSC99-2218-E-001-006 The first author also sincerely acknowledges the academic committee of the Taiwan Geosynthetics Society who give her this precious opportunity to participate in this great event.

REFERENCES

AASHTO, (2002). Standard Specifications for Highway Bridges, American Association of State Highway and Transportation Officials, 17th Edition, Washington, DC, USA, 689 p

Allen, T.M.; Bathurst, R.J.; Holtz, R.D.; Walters, D.; Lee, W.F. (2003). A new working stress method for prediction of reinforcement loads in geosynthetic walls. Canadian Geotechnical Journal,40(5): 976-994

Bathurst, R.J., Miyata, Y., Nernheim, A. and Allen, T.M. (2008). Refinement of K-Stiffness method for geosynthetic reinforced soil walls, Geosynthetics International, 15(4): 269–295

Bathurst, R.J., Vlachopoulos N., Walters, D.L., Burgess, P.G., and Allen, T.M. (2006). The influence of facing stiffness on the performance of two geosynthetic reinforced soil retaining walls. Canadian Geotechnical Journal, 43(12): 1225-1237

Bathurst, R. J., Allen, T. M. and Walters, D. L. (2005). Reinforcement loads in geosynthetic walls and the case for a new working stress design method. Geotextiles and Geomembranes, 23(4): 287–322.

Elias, V., Christopher, B.R., and Berg, R.R., (2001). Mechanically Stabilized Earth Walls and Reinforced Soil Slopes Design and Construction Guidelines. Report No. FHWA-NHI-00-043, National Highway Institute, Federal Highway Administration, Washington, D.C. March

Hatami, K and Bathurst R. J.(2006). Numerical model for reinforced soil segmental walls under surcharge loading. Canadian Geotech Journal, 67(4): 1066-1085

Hatami, K and Bathurst R. J.(2005). Development and verification of a numerical model for the Analysis of geosynthetic-reinforced soil segmental walls under working stress conditions. JGGE, 132(6): p 673-684

Huang B., Bathurst R. J. and Hatami, K (2009). Numerical study of reinforced soil segmental walls using three different constitutive soil models. JGGE,135(10):1486-1498

Holtz, Robert, (2010). Reinforced soil technology: from experimental to the familiar. Proc. 46th Karl Terzaghi Lecture, Geo-Institute of American Society of Civil Engieers, GeoFlorida Conference, West Palm Beach, Florida.

Karpurapu, R.G., and Bathurst, R.J. (1995). Behaviour of geosynthetic reinforced soil retaining walls using the finite element method. Computers and Geotechnics, 17(3): 279–299.

Leshchinsky, D. (2010). Geosynthetic reinforced walls and steep slopes: Is it magic. Geosynthetics Magazine, 28(3): pp16-24

Leshchinsky, D. (2009). On global equilibrium in design of geosynthetic reinforced wall. JGGE, ASCE, 135(3): 309-315

Ling, H.I., Cardany, C.P., Sun, L.-X., and Hashimoto, H. (2000). Finite element study of a geosynthetic-reinforced soil retaining wall with concrete-block facing. Geosynthetics International, **7**(3): 163–188.

Lopes, M.L., Cardoso, A.S., and Yeo, K.C. (1994). Modelling performance of a sloped reinforced soil wall using creep function. Geotextiles and Geomembranes, 13:181–197.

National Concrete Masonry Association, (2010). Design Manual for Segmental Retaining Walls. Bathurst, R.J., Editor, 3rd Ed. Herndon, Virginia, U.S.A., 282p.

PLAXIS. (2005). Plaxis Finite Element Code for Soil and Rock Analyses, Version 8.2, P.O. Box 572, 2600 AN Delft, The Netherlands (Distributed in the United States by GeoComp Corporation, Boxborough, MA).

Zornberg, J.G., Sitar, N., and Mitchell, J.K. (1998). Limit equilibrium as basis for design of geosynthetic reinforced slopes. Journal of Geotechnical and Geoenvironmental Engineering, ASCE, 124(8): 684-698.